Prism effects on total station measurements: steps towards computational correction

Andreas Wieser[1] (ORCID), Robert Presl[2] (ORCID), Lucas Dammert[3] (ORCID), Tomas Thalmann[3] (ORCID) & Hans Neuner[3] (ORCID)

[1] ETH Zürich, wiesera@ethz.ch (corresponding author)
[2] ETH Zürich
[3] TU Wien

DOI: 10.3217/978-3-99161-070-0-019, CC BY 4.0

Abstract

Systematic effects on total station measurements arising from solid glass corner cube prisms can lead to deviations at the mm-level. We show that these deviations can be mitigated by forward modeling based on geometrical optics and assumed properties of the reflectors, or by empirical modeling based on calibration measurements with a variety of reflector poses. Establishing the forward model is less costly, but some empirical modeling is required to derive necessary pa-rameters which are not disclosed by the manufacturers. Empirical modeling can better account for specific deviations of individual prisms and for deviations related to the particular data pro-cessing within a total station. Corrections obtained by modeling are applicable to measurements of moving prisms, e.g., for tracking drones or construction machines, and to geodetic network measurements where differences exceeding 5 mm could result from uncorrected prism effects even when using high-precision single prisms.

1 Introduction

Precise distance and angle measurements using a total station typically require a retro-reflective prism as signalization of the target point. In surveying, solid glass corner cubes are normally used for this purpose; see e.g., Rüeger (1996). Refraction at the prism's front face and the lower propagation speed inside the glass significantly affect distance and angle measurements. An additive constant can compensate for these effects only if the prism is perfectly aligned with the incoming line-of-sight (LoS). With other prism orientations, and in particular when using prism assemblies like a 360-degree reflector, systematic deviations at the level of several mm can arise, see e.g., Heister (1998), Favre und Hennes (2000), Braun (2015), Lackner and Lienhart (2016). These effects can surpass the quality specifications of the reflectors and arise from their *use*, particularly with large angles of incidence (AOI) of the measurement beams onto the prisms.

For laser tracker measurements, hollow corner cube prisms are typically used nowadays, i.e., prisms with orthogonal reflective surfaces but air instead of glass in front of them, or only a thin protective layer of glass. Such reflectors are usually too expensive and not robust enough for use in surveying. Other means of mitigating deviations due to the reflector are needed. The effects are smaller for reflectors with smaller prisms, and manufacturers have developed reflectors that minimize certain effects over relatively large ranges of reflector orientations, see e.g. Bernhard

et al. (2008). Nevertheless, the effects can limit the accuracy in practical applications. Due to their systematic nature, it is in principle possible to mitigate them.

We show that compensation by forward modeling based on geometrical optics and assumed properties of the prisms and reflectors is possible, or by empirical modeling based on calibration measurements with a variety of prism poses. Establishing the numerical forward model is less costly, but some empirical modeling is required to derive necessary parameters of the prisms and total station which are not disclosed by the manufacturers. Empirical modeling, on the other hand, can better account for specific deviations of individual prisms (rather than prism types) and for deviations related to the particular data processing within a total station, especially in relation to image-based angle measurements (e.g., ATR for Leica instruments).

The present study has not yet provided a comprehensive solution of the problem. However, encouraging results were achieved with relatively simple calculations, and priorities for further development can be identified using these results. Corrections obtained by modeling as presented herein are applicable to tasks with moving reflectors, e.g., for tracking drones, tilted INS-based poles, and to geodetic network measurements where differences exceeding 5 mm could result from uncorrected prism effects and be forced into observation residuals, primarily of horizontal and vertical angles, even when using high-precision single prisms.

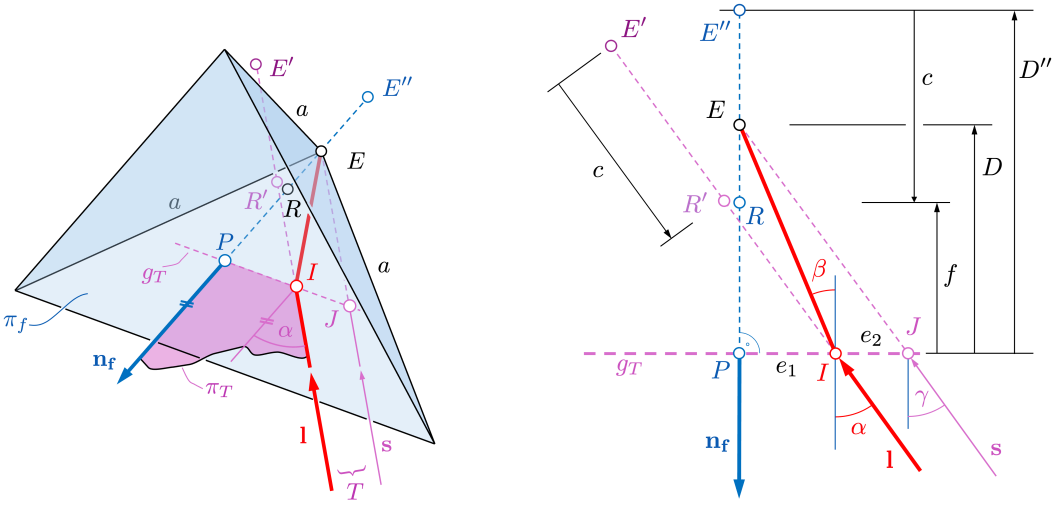

Fig. 1: Geometry and key elements of a corner cube prism with a principal ray (red) incident under an angle-of-incidence α from position T (left); key elements in plane π_T (right).

2 Theoretical forward modeling

The idea of forward modeling is to assume the position and orientation of a reflector $\mathscr{R}$ relative to the total station $\mathscr{T}$ as known, calculate the beam path using geometrical optics, and determine the deviations of the apparent target point R' from the reflector's true reference point R.

A corner cube prism is obtained by cutting a cube of glass into a triangular pyramid with an equilateral triangle as its base. We follow the terminology used by Peck (1948): The base is the *front face* π_f of the prism (see fig. 1, left). We denote the equal lengths of the orthogonal edges

from the *corner* E to π_f as a, and the orthogonal projection of E onto π_f as *pole* P. The *depth* D of the prism, i.e., the distance $\overline{EP}$ is $D = a/\sqrt{3}$. The outward pointing unit normal vector of π_f is $\mathbf{n}_f$, and the line through E and P, parallel to $\mathbf{n}_f$, is the *prism axis*. Real prisms for surveying are often cut out further, e.g., to have a round front. For our purposes, it is sufficient to represent this by a mask at the triangular front face and by calculating only beams that enter and leave the prism through the transparent part of this mask.

Typically, distances measured using EDM and a reflector are corrected by an additive (reflector) constant c such that they refer to R. However, a fixed value is not sufficient to achieve this correction for all prism orientations. Manufacturers take this into account by choosing glass with an appropriate refractive index (below 1.5 to above 1.7), mutually adapting the size of prisms, the geometry of the reflector, and the (typically negative) value of c such that the impact of the prism on the measured distances is negligible over a certain range of orientations. The choice can be such that R is obtained if the prism face is (nearly) orthogonal to the EDM measurement beam (AOI$=0$). For this case, and assuming that R lies on the prism axis at a distance f behind the front face (see fig. 1), this means (see e.g., Rüeger, 1996):

$$c = f - D \cdot \frac{1}{n_{\mathrm{G}}}. \tag{1}$$

In eq. (1), the group index of air has been neglected. Only n_{G}, the one of the glass at the EDM wavelength needs to be taken into account. Surveying prisms are often coated. This has an impact on the noise level of the measurements and the deviations modeled herein. However, we neglect this, herein, and leave potential related improvements of the model for later.

Each *incident ray* reaching the front face under a suitable angle and at a suitable location will be reflected three times within the prism—once on each of the orthogonal internal faces—, and leave it as *emanating ray* at a different location but parallel to the incident ray. Unless stated otherwise, we will subsequently only refer to such parallel rays as incident and emanating, and we will assure not to use others for the calculation. All parallel incident rays have the same path length within the prism, see e.g., Rüeger (1996). We can study the impact of a prism on total station measurements by analyzing the path of the *principal ray*, i.e., the incident ray which enters and exits at the same point I.

Figure 1 shows the situation for a principal ray reaching the prism in the direction of a unit vector $\mathbf{l}$ from a total station at T. The ray intersects π_f at an incidence angle α in point I and changes direction according to Snell's law. It reaches E directly along the straight line from I and returns to T along the same path. The point I where it enters and leaves the prism is the *principal point* for the direction $\mathbf{l}$. The incident ray, the refracted ray and the normal vector of the interface lie in a plane (Mahajan, 2014, p. 15). We denote it as π_T. Also, E, P, T and the intersection J of the straight line from T to E lie in π_T. This allows us to study the refraction at the front face in this plane, i.e., in 2D, see fig. 1 (right).

If T were on the prism axis, we would have $I = P$ and the ray would cover the distance D within the prism. Since the refractive index n_G of the glass differs from the one in air, this distance would appear as $D'' = n_{\mathrm{G}}/n_{\mathrm{air}} \cdot D$, and the total station would yield the coordinates of the apparent corner E''. Adding the reflector constant would move E'' along the prism axis. If the reflector's reference point R is also on the prism axis, using the value of c as of eq. (1) would correct the distance such that the calculated point is R instead of E''.

However, if the prism axis does not point exactly to the total station, the situation is more complicated. The principal point is not known beforehand. It is on g_T between J and P, but its distances e_1 and e_2 from these two points need to be calculated. Given $\mathbf{x}_T$, $\mathbf{x}_R$, and $\mathbf{n}_f$ in the same coordinate frame, we can calculate $\mathbf{x}_P$ and $\mathbf{x}_J$ in that frame, as intersections of the prism axis and the chord TE with π_f. The angle of incidence γ in J can be calculated from $\mathbf{n}_f$ and the unit vector $\mathbf{s}$ pointing from T to E; it serves as an approximation $\alpha^{(0)}$ of the AOI in I:

$$\gamma = \arccos(-\mathbf{n}_f^T \cdot \mathbf{s}) := \alpha^{(0)} \tag{2}$$

If T is far from the prism, α will practically be equal to γ. To also account for other situations, we calculate α and I by iteration using Snell's law, the unit vector $\mathbf{e}$ between P and J, and the geometrical situation depicted in fig. 1:

$$\beta^{(i)} = \arcsin\left(\frac{n_{\text{air}}}{n_{\text{G}}} \cdot \sin\alpha^{(i)}\right) \approx \arcsin\left(\frac{1}{n_{\text{G}}} \cdot \sin\alpha^{(i)}\right) \tag{3}$$

$$e_1^{(i)} = D \cdot \tan\beta^{(i)} \tag{4}$$

$$\mathbf{x}_I^{(i)} = \mathbf{x}_P + e_1^{(i)} \cdot \mathbf{e} \tag{5}$$

$$\mathbf{l}^{(i)} = \frac{\mathbf{x}_I^{(i)} - \mathbf{x}_T}{||\mathbf{x}_I^{(i)} - \mathbf{x}_T||} \tag{6}$$

$$\alpha^{(i+1)} = \arccos(-\mathbf{n}_f^T \cdot \mathbf{l}^{(i)}) \tag{7}$$

In our later calculations, we terminate the iterations when α changes by less than 10^{-6} rad, which corresponds to sub-micrometer accuracy for e_1 and I. We then check whether I, as obtained from eq. (5) in the last iteration, lies within the transparent part of the front face mask. If not, the prism cannot be measured from T for the given relative position and orientation.

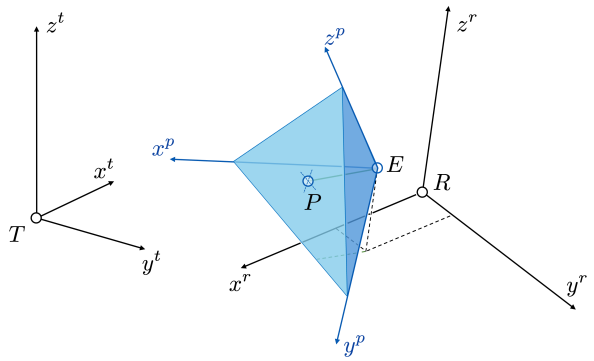

Fig. 2: Coordinate frames used for the calculations: total station's topocentric frame (t-frame), reflector frame (r-frame), ans prism frame (p-frame) for a reflector with a single prism.

The total station's angle measurements represent the direction of $\mathbf{l}$. The calculated ('apparent') target point lies in that direction from I. Without c added, it is the apparent prism corner E'; with c added ($c < 0$) to the distance measurement, it is R'. The deviations of the measurements follow as the differences between R' and R. Herein, we define them as 'expected/observed minus true' and quantify them in terms of distance, horizontal angle, and zenith distance. For plotting and assessing, we convert the angular deviations to metric ones, because the impact of the prism orientation on the angles is actually an apparent eccentricity of the target.

Ultimately, we need the coordinates of R' and R in the total station's left-handed Cartesian coordinate frame (t-frame). For convenience, we model the reflector through its own left-handed

Cartesian frame (r-frame) with origin in R and axes aligned with distinct directions on the reflector, such that its orientation relative to the total station can easily be expressed using a rotation matrix $\mathbf{R}_r^t$ or an axial vector $\boldsymbol{\psi}_r^t$ (e.g., Euler angles). Finally, we associate the prism with a right-handed Cartesian frame (p-frame) whose origin is in E and whose axes coincide with the orthogonal edges of the prism. The prism's pose in the reflector is then represented by $\mathbf{x}_E^r$ and $\mathbf{R}_p^r$. Fig. 2 shows these frames for a reflector with one prism. Without loss of generality, we carry out the above iterations in the p-frame.

Reflector with single prism

For forward modeling in case of a reflector with a single prism we choose appropriate values for the prism depth D, for n_G as a function of wavelengths (e.g., as a look-up table), for the prism's orientation $\boldsymbol{\psi}_p^r$ and corner $\mathbf{x}_E^r$ in the r-frame, and for the front face mask. All this defines the reflector $\mathscr{R}$. Then, the position $\mathbf{x}_R^t$ and orientation $\boldsymbol{\psi}_r^t$ of the reflector in the t-frame must be defined, and finally the relevant details of the total station $\mathscr{T}$. Herein, the latter comprise only the EDM carrier wavelength, the wavelength of the target illumination used for angle measurement, and the reflector constant c.

As an example, we present results for a Leica standard prism (GPH1) and mini prism (GMP101) 'measured' from 30 m distance using a hypothetical total station with different wavelengths, chosen to highlight the sensitivity w.r.t. prism size and wavelengths, see fig. 3. The parameters of the prisms are given in tab. 1. The reflector is rotated stepwise from -60 to 60 gon about its vertical axis while R and T remain at the same height. The deviations increase with AOI (here: magnitude of rotation). They stay below 1 mm for distances with AOI up to 40 gon and hardly exceed 2 mm even at the extremes. However, they reach 7 mm horizontally and 4 vertically. The deviations are 50% smaller for the smaller prism. The angular deviations are practically independent of the wavelengths but the distance deviations depend strongly on the EDM wavelength because the fixed value of c is appropriate for only one specific wavelength. So, while—in the forward modeling as in the real world—the additive constant must be properly chosen for the specific combination of instrument and reflector, the above calculations can be carried out using only the group refractive index n_G of the EDM.

Reflector with multiple prisms

To model a reflector $\mathscr{R}$ with more than one prism, e.g., a 360-degree reflector, each prism (p_k) must be defined in terms of D_k, n_{G_k}, front mask, $\mathbf{x}_{E_k}^r$ and $\boldsymbol{\psi}_{p_k}^r$, and the apparent target points R'_{p_k} of these prisms, calculated exactly as above, must be combined into an overall target point $R'_{\mathscr{R}}$. That combination should resemble the measurement process of the total station.

It is hard to imagine that the individual prisms would contribute to the distance other than through a weighted average, where the weights correspond to the signal power returned by the individual prism and thus to the position of the prism within the EDM beam profile, the AOI and the area of the respective front face through which emanating rays reach the total station (*active area*). Also for the angle measurements the overall result will likely be a weighted average of the angles corresponding to the individual prisms, but the weights could depend on additional parameters (e.g., in case of advanced image processing within the total station), or could be 0

for all but one prism (e.g., if the angle measurement beam is narrowly focused or the image processing distinguishes the prisms).

Herein, we take a simple approach by averaging the R'_{p_k} with weights proportional only to the active area of the prisms. We thus neglect the potential impact of the power distribution within the beams, of the pointing by the total station, and of potential advanced image processing within the total station. The results indicate, that already this simple model yields astonishing agreement between forward modeling and real measurements, see sec. 3.

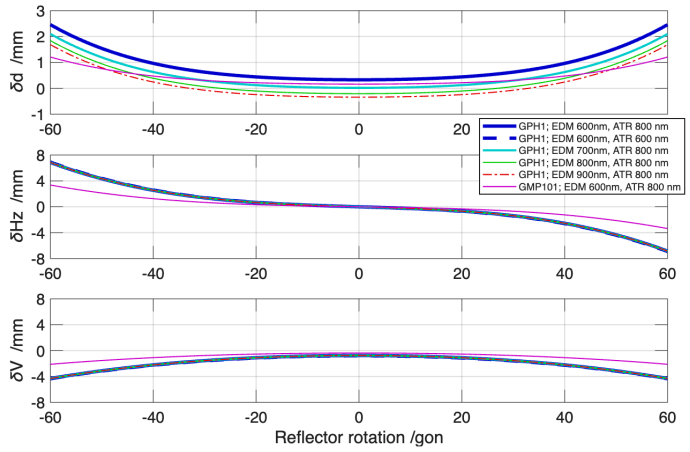

Fig. 3: Simulated deviations for an upright Leica standard and mini prism (GPH1,GMP101) with various combinations of assumed wavelengths of EDM and targeting (ATR); different azimuthal rotations relative to the total station.

3 Empirical modeling

The deviations can also be determined experimentally. For full empirical modeling, measurements need to be made with a sufficiently large variety of distances and 3d orientations of the reflector to enable interpolation for arbitrary configurations. Such modeling would account for most or all factors so far neglected in the above forward model and would thus be potentially more accurate. However, it is costly to establish and requires appropriate filtering to mitigate the impacts of measurement noise.

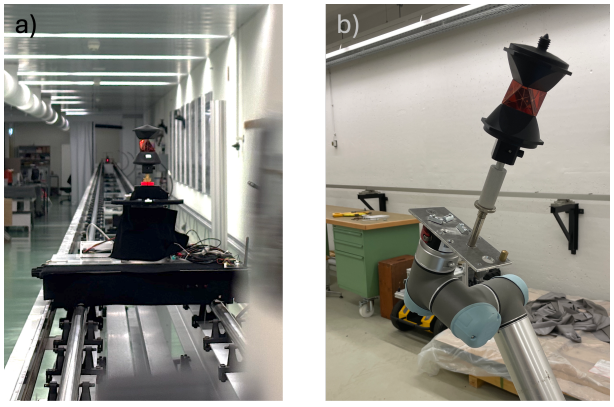

Fig. 4: Lab setups for empirical determination of prism effects: (a) rotation table on trolley of horizontal comparator (ETH Zürich), (b) prism mounted on industrial robot (TU Wien).

Instead of aiming for a full empirical model, we use a small set of experiments herein to assess the quality of the results from the forward model and to identify needs and potential for its further development. We carried out measurements with a Leica TS60 and various reflectors on

the horizontal comparator bench in a lab at ETH Zürich, see fig. 4a, and with a Leica MS60 and various reflectors on an industrial robot (Universal Robots UR5 collaborative robotic arm) in a lab at TU Wien, fig. 4b.

Figure 5a shows results with a Leica GPH1 reflector at a distance of 30 m from the TS60. The prism's front face was vertical, the TS60 and the reflector were at the same height, and the reflector was rotated about its standing axis in steps of 1 deg within ±65 deg (0: AOI= 0; > 0: clockwise, as seen from top). At each step, 10 measurements were recorded. The figure shows the deviations of the original measurements (gray dots) and their mean (blue line) from the mean value at rotation 0. The predictions from the forward model (parameters see tab. 1) are plotted as dashed red lines; the thin, solid red lines are obtained when predicting for a 4gon lower rotation angle, e.g., to account for an undetected initial misalignment of the setup.

Simulation and measurements differ by less than 0.5 mm for AOI up to 40 deg and about 1 mm for larger AOI. The predicted horizontal deviations fit almost perfectly when assuming the misalignment of −4gon. However, the predicted distances fit almost perfectly when *not* assuming this misalignment. We do not yet know the reasons for this discrepancy; possibly they are related to geometric deviations of the reflector, similar to the ones studied in Lösler et al. (2026).

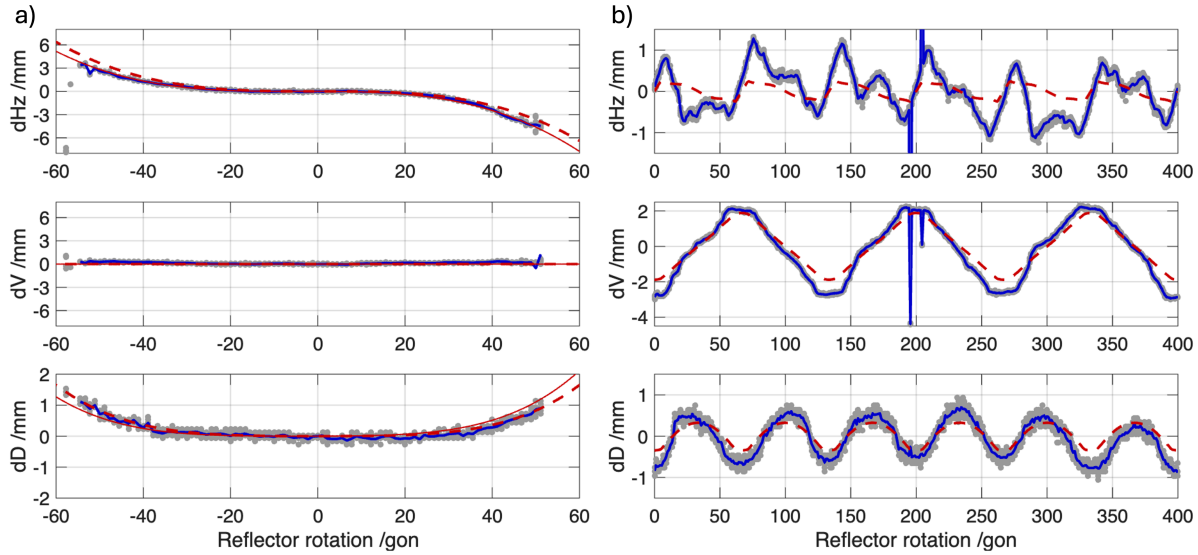

Fig. 5: Predicted and observed deviations of total station measurements on reflectors for different rotation (no tilt); GPH1 (a), GRZ4 (b).

Fig. 5b shows similarly obtained empirical and predicted deviations for a Leica GRZ4 reflector in upright position, 30 m from the total station, and with clockwise rotation by 400 gon. Based on the reflector design (6 prisms, alternately flipped upside down and tilted up-/downwards) we expected that the deviations exactly repeat every 120 deg (133 gon) for the angles and every 60 deg for the distances. We see this, within about 0.3 mm, for the distances and the vertical angles, but the pattern of the horizontal deviations differs by up to about 1 mm from this repeatability. Sub-mm accuracies of calculated corrections, if possible at all for such reflectors, would likely require adaptation to the individual prism, not just prism type. The figure also shows outliers at specific orientations, a similar effect as the one shown and discussed in Lackner and

Table 1: Parameters used for forward modeling of various reflectors. Except c, these values are assumptions and may not correspond to the true values, which are not directly observable and not publicly available.

Reflector	D /mm	$\mathbf{X}_E^r$ /mm	n_G @ 658 nm[a]	c /mm[b]	Comments
GPH1	39.55	−13.35|0|0	1.535	−34.4	Size determined for $\delta D(\mathrm{AOI}=0) \stackrel{!}{=} 0$ with $c = 34.3$ mm
GMP101	19.33	−6.56|0|0	1.535	−16.9	GPH1 scaled to yield $c = 34.4 - 17.1$ mm
GRZ4	19.19	0|0|0	1.535	−11.3	Size from outside dimensions and assumed $\mathbf{X}_E^r$
GRZ122	18.19	3.46|0|2.45	1.700	−11.3	D, $\mathbf{X}_E^r$ and n adapted to outside dimensions and $\overline{\delta D} = 0$[c]

[a] Except for GRZ122 the refractive index of BK7 glass according to Rüeger, 1996 was used. Only the group index for the EDM wavelength of the TS60 is reported here. For GRZ122 n was assumed constant; according to Bernhard et al. (2008), the actual value is likely even higher than 1.7.

[b] These are absolute prism constants; Leica typically reports the constants relative to GPH1, i.e., $c + 34.4$ mm.

[c] $\overline{\delta D} = 0$ indicates the average distance deviation over 360 deg rotation of the vertical prism, with $c = -11.3$ mm.

Lienhart (2016). Such errors can almost certainly not be predicted with sufficient accuracy for compensation, but the model can be used to identify the AOI and the principal point on each prism of the reflector and thus to detect situations in which large deviations are more likely than in others; this can be used as an information for weighting observations in subsequent processing.

We used an industrial robot for measurements with a Leica GRZ122 reflector tilted from −35 to 35 deg (towards/away from the total station) and rotated between 0 and 355 deg about the tilted axis. The distance was about 25 m. The reference point R remained at the same height as the total station for all orientations. Rotation and tilt were incremented in steps of 5 deg. Measurements were carried out automatically at each orientation. For determining the deviations, each pose of the 360-degree prism was revisited with the robotic arm and a standard round prism, manually aligned in the direction of the total station. The deviations of the polar coordinates, derived from these measurements, thus include the uncertainties of the reference measurements and of the repeatability of the robotic arm (0.1 mm according to the specification).

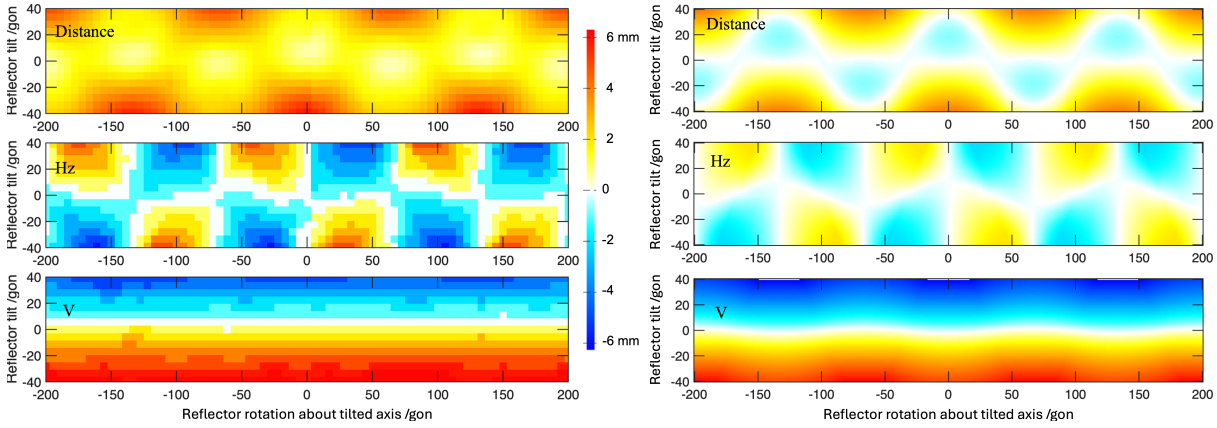

Fig. 6: Deviations (measured minus expected) of total station measurements on Leica GRZ122 for different tilt and rotation (left: measurements; right: forward model).

The results are visualized in fig. 6 (left). The circular repeatability of the deviation patterns with prism rotation is plausible given the specific assembly of the six prisms on this reflector. It is

obvious that the deviations in azimuth and zenith distance increase in magnitude with increasing tilt, exceeding 6 mm in extreme cases.

Despite small differences, particularly in absolute magnitude, the predicted deviations from the forward model, fig. 6 (right), match the empirical results well. The differences are likely due to the simplifying assumptions regarding the total station's measurement process, the geometry and refractive index of the prism (see tab. 1), but also to remaining uncertainties of the experimental measurements and chosen reference values. Nevertheless, the results indicate that it may be possible to practically compensate a large part of the prism effects by numerical modeling.

4 Compensation of effects

The above theoretical and empirical models represent the deviations $\delta\mathbf{p}$ of the total station measurements, in the sense 'expected minus true', as a function of the true coordinates $(\mathbf{x}_R^t)^{\text{true}}$ and orientation $(\psi_r^t)^{\text{true}}$ of the reflector relative to the total station:

$$\delta\mathbf{p} := [\delta D, \delta Hz, \delta Zd]^T = \mathbf{f}_{\mathscr{T},\mathscr{R}}\big((\mathbf{x}_R^t)^{\text{true}}, (\psi_r^t)^{\text{true}}\big). \tag{8}$$

Given a reasonable approximation $(\psi_r^t)^{\text{aprx}}$ of the reflector's orientation, the function $\mathbf{f}_{\mathscr{T},\mathscr{R}}$ for the specific (type of) reflector $\mathscr{R}$ and total station $\mathscr{T}$ can be used to mitigate the prism effects on the measurements $\mathbf{p}^{\text{raw}}$ output by the total station:

$$\mathbf{p}^{\text{corr}} = \mathbf{p}^{\text{raw}} - \mathbf{f}_{\mathscr{T},\mathscr{R}}\big((\mathbf{x}_R^t)^{\text{corr}}, (\psi_r^t)^{\text{aprx}}\big). \tag{9}$$

It may be sufficient to evaluate eq. (9) with the reflector coordinates $(\mathbf{x}_R^t)^{\text{raw}}$, directly corresponding to the raw total station measurements, instead of the 'corrected' ones, $(\mathbf{x}_R^t)^{\text{corr}}$, which need $\mathbf{p}^{\text{corr}}$ for calculation. However, a refined approach may need solving eq. (9) iteratively. The necessary approximation of the reflector's orientation can, e.g., be derived from the deliberate choice how a reflector is oriented relative to the network points in a static set-up or from the pose estimation of a kinematic platform on which the reflector is rigidly mounted.

The above models can also be used for weighting of total station observations within further data processing, be it for geodetic network adjustment, for checking coordinates of individual points, or for trajectory estimation. For this, the AOI and the location of the principal point $\mathbf{I}$ within each prism's front face can be used as indicators of the expected quality of the measurements. Measurements obtained with AOIs at which outliers are likely, measurements with the LOS intersecting the prism close to the edge between adjacent prisms of a 360-degree reflector, or measurements obtained in configurations for which the model $\mathbf{f}_{\mathscr{T},\mathscr{R}}$ is more uncertain, can be downweighted relative to other observations.

5 Conclusions

The use of glass prisms as reflectors for total station measurements introduces systematic deviations if the line-of-sight and the reflector are not perfectly aligned or if the additive constant does not match the reflector and the carrier wavelength of the EDM. These effects have long been known and studied. Herein, we presented an analytical forward model to predict the deviations

for arbitrary reflectors and geometric configurations. The model can handle single-prism reflectors as well as prism-assemblies like 360-degree reflectors. It can deal with arbitrary distance and orientation of the reflector relative to the total station.

We have carried out measurements for the empirical determination of the deviations, stepwise turning reflectors into various orientations. The model predicts the deviations—up to several mm laterally and vertically—and their dependence on reflector orientation to within 1 mm or better. However, its evaluation requires parameters typically not disclosed by the reflector manufacturers, e.g., prism dimensions and refractive index, and it does not account for imperfections of the prisms and reflector assembly, e.g., misalignments, inhomogeneities or scattering of light at the edges. Finally, it also does not yet account for the actual measurement process within the total station, e.g. the beam profiles and divergence, or the internal data processing.

Some of the above parameters can be inferred from experimental data with sufficient accuracy, others would require individual calibration of the prism-total-station system, and some would likely appear random or too variable in time for effective modeling. We will address this in the future. Overall, we expect that forward modeling can be a viable and economically attractive solution to mitigating prism effects, particularly for application cases where reflectors cannot be carefully aligned towards the total station.

Literature

BERNHARD, H., HINDERLING, J. & PETERMANN, M. (2008): Zielobjekt zur Retroreflexion einer optischen Strahlung. Patent, WO2008043436A1.

BRAUN, J. (2015): Testing of the automatic targeting of total station Trimble S8 on reflective targets. In Proc.: 5th International Multidisciplinary Scientific GeoConferences SGEM2015, 491–498.

FAVRE, C. & HENNES, M. (2000): Zum Einfluss der geometrischen Ausrichtung von 360°-Reflektoren bei Messungen mit automatischer Zielerfassung. In: Vermessung, Photogrammetrie, Kulturtechnik (VPK) (2), 72-–78.

HEISTER, H. (1998): Zur Fehlausrichtung von Tripelprismen. In: Zeitschrift für Ver- messungswesen (ZfV) (113), 249–258.

LACKNER, S. & LIENHART, W. (2016): Impact of Prism Type and Prism Orientation on the Accuracy of Automated Total Station Measurements. In: Proc. Joint Intl. Symposium on Deformation Monitoring (JISDM), 8 pp.

LÖSLER, M., KOPITZKE, K.-L. & ESCHELBACH, C. (2026): On the suitability of spherical glass-body reflectors in industrial applications. In: Lienhart, W. (Ed.) Ingenieurvermessung 2026 – Beiträge zum 21. Internationalen Ingenieurvermessungskurs, Graz, Verlag der Technischen Universität Graz, 158–169.

MAHAJAN, V.N. (2014): Fundamentals of Geometrical Optics. SPIE, ISBN: 978-0819499998.
PECK, E.R. (1948): Theory of the Corner-Cube Interferometer. In: Journal of the Optical Society of America (38), 1015–1024. RÜEGER, J.M. (1996): Reflectors. In: Electronic distance measurement: an introduction. 4th ed., Springer Verlag, ISBN: 978-3-540-61159-2, 148–164.